RECEIVE ANTENNA IMPACT ON SPATIO-TEMPORAL AVAILABILITY IN SATELLITE-TO-INDOOR BROADCASTING

Marko Milojević, Giovanni Del Galdo, Nuan Song, Martin Haardt

Ilmenau University of Technology,
Communications Research Laboratory,
P.O. Box 100565, 98684 Ilmenau, Germany
marko.milojevic@tu-ilmenau.de

Albert Heuberger

Fraunhofer Institute Integrierte Schaltungen IIS
Am Wolfsmantel 33, 91058 Erlangen, Germany
albert.heuberger@iis.fraunhofer.de

ABSTRACT

This contribution studies spatio-temporal availability in satellite-to-indoor broadcasting. The performance of both theoretical and measured single and multiple antenna receivers with various polarimetric radiation patterns is compared for different satellite elevation angles. The spatio-temporal satellite to indoor channels are obtained via a 3D ray tracing engine and a geometry-based channel modeling tool. Moreover, the influence of coupling effects between closely spaced antennas on the availability is studied. Under the assumption of a Line-Of-Sight (LOS) connection between the satellite and the wall where the possible window is placed, the indoor performance with and without windows is compared. The results show quantitatively that additional antennas placed at the receiver reduce both the spatial and the temporal variability of the received power, significantly reducing the transmit power required for the same target availability. The antenna coupling effects increase the required link margin.

1. INTRODUCTION

Satellite broadcasting systems are attractive due to a possible coverage of large areas. Some satellites, such as XM Radio, offer link margins of up to $18\,\mathrm{dB}$ which makes indoor reception already feasible. For future satellite systems, a significant increase of the Effective Isotropic Radiated Power (EIRP) is planned, which will allow indoor reception of the satellite signals with high availability for broadband services. Since in mobile reception only time diversity (using long interleavers) has been employed so far, there is still some room for improvement in stationary or portable reception in indoor environments by using spatial or polarization diversity. The characterization of the propagation environment is very important for the planning of satellite communication systems. To characterize the satellite-to-indoor channels, either measured channels or channels obtained by deterministic channel models such as ray-tracers can be analyzed. In the literature, only a few satellite-to-indoor measurements are discussed dealing with the performance of different receive antenna strategies, polarization diversity, and the influence of moving persons or objects.

In [1], it is concluded that the wall attenuation influences mostly the indoor coverage in the range of 1.1 GHz - 1.6 GHz. Within the MAESTRO project [2], [3], satellite-to-indoor measurements in the L-band have been carried out in Erlangen and Athens by using the Worldspace Afristar satellite having an EIRP of $48\,\mathrm{dBW}$. It is concluded that the percentage of positions within the room from which a satellite signal can be received with good quality is in the range of $30\ \%$ up to $80\ \%$ with corresponding link margins of $10\,\mathrm{dB}$ to $16\,\mathrm{dB}$. Measurement results in [4] show that the received electromagnetic field is strongly diffused in the interior of a building. In [5], it is shown that the polarization state of the propagation wave changes significantly inside the room.

In this paper we extend the investigations carried out in [6] and [7] with respect to the temporal variation, elevation, additional antenna configurations, coupling effects, and the influence of the windows. This paper is organized as follows: in Section 2 we describe our deterministic channel modeling concept. In Section 3, we discuss the influence of different antenna configurations, polarizations, elevations, temporal variations of the channel, coupling effects, and windows on the satellite-to-indoor link availability for realistic link margins. In Section 4 the conclusions are drawn.

2. SATELLITE-TO-INDOOR CHANNEL MODEL

Fig. 1 shows the flowchart of the satellite-to-indoor channel modeling framework. The satellite-to-indoor channel coefficients are obtained by combining the 3D ray-tracing simulation tool WinProp[1] to obtain the information on the propagation paths for the defined scenario and the IlmProp[2] [8], a flexible geometry-based MIMO channel modeling tool for wireless communications, to create the channels for various

[1] http://www.awe-communications.com
[2] http://www.tu-ilmenau.de/nt/en/ilmprop

978-1-4244-1757-5/08/$25.00

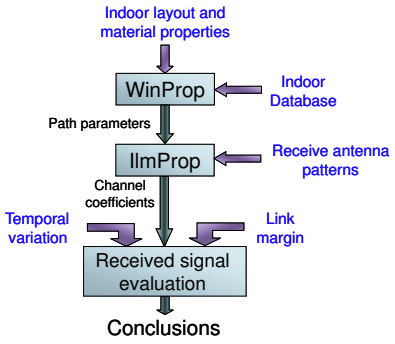

Fig. 1. Block diagram of our analysis

antenna configurations. In [9], [10], and [11] WinProp has been validated with the help of measurements. WinProp takes into account transmission, reflection, and diffraction. After the satellite-to-indoor scenario is defined and modeled by the WinProp, the path strength and spatial information of each path is fed to the IlmProp. The trajectory of each path is modeled by means of point-like scatterers which represent points of interaction. The IlmProp supports different receive antenna patterns and allows us to compare their performance. In our simulations, a left-hand circularly polarized satellite signal with carrier frequency 2.0 GHz is received by a stationary indoor receiver. The polarization for Non-Line-Of-Sight (NLOS) paths becomes random due to diffractions and reflections, while the LOS component is set to be Left Hand Circularly Polarized (LHCP). In fact, in [4], it is concluded that in the satellite-to-indoor scenario the electromagnetic field is diffuse and the circular polarization is not preserved in the far field away from the window. In [6], more details on the deterministic channel modeling components can be found. Additionally, we take into account temporal variations of the receive power due to the man movement in the vicinity of the receiver. The parameters characterizing man movement are obtained from the satellite-to-indoor measurements. The person movement, without blocking the incoming signal, increases the received signal standard deviation in all available data sets. The Probability Density Function (PDF) of the difference between the received power in measurements with and without person movement is well approximated by the PDF of a truncated normal distribution with zero mean and standard deviation in the range from $0.7\,\mathrm{dB}$ up to $1.5\,\mathrm{dB}$, depending on the environment, as reported in [7]. In the following, the PDF of a truncated normal distribution with zero mean, a standard deviation of $0.9\,\mathrm{dB}$, and truncation at $\pm 2.3\,\mathrm{dB}$ is used.

3. PERFORMANCE COMPARISON OF DIFFERENT RECEIVE ANTENNAS

In this section we compare the performance of different receive antenna schemes with respect to the Cumulative Distribution Function (CDF) of the fade depth. We study a room oriented towards the satellite, i.e., there is a LOS between the satellite and the window. The carrier-to-noise ratio at the receiver, denoted by C/N, is defined as the difference between the received signal power C and the received noise power N, i.e.,

$$C/N = C - N \quad [\mathrm{dB}]. \tag{1}$$

The value of the Fade Depth FD is estimated as the difference between a reference carrier-to-noise ratio C/N_{ref} and the carrier-to-noise ratio at the receiver C/N, i.e.,

$$FD = (C/N_{\mathrm{ref}} - C/N) \quad [\mathrm{dB}], \tag{2}$$

where C/N_{ref} refers to a position outside of the room in a pure LOS regime. The Link Margin LM is defined as the difference between the reference carrier-to-noise ratio C/N_{ref} and the minimum carrier-to-noise ratio C/N_{min} needed for good reception of the signal, i.e.,

$$LM = (C/N_{\mathrm{ref}} - C/N_{\mathrm{min}}) \quad [\mathrm{dB}]. \tag{3}$$

If the fade depth is higher than the link margin we say that the communication link is *not available*, otherwise it is *available*. In Fig. 2 we show the predicted average receive signal power in the room for a satellite elevation of 40° and an azimuth φ of 45°. There are three different areas of receive signal power that are denoted as $\mathcal{A}$, $\mathcal{B}$, and $\mathcal{C}$ in Fig. 2:

- The area $\mathcal{A}$ is dominated by the LOS channel component impinging through the window. The fade depth is low and exhibits a very low spatial variation. As a result, a very high availability is achieved.
- The area $\mathcal{B}$ is characterized by rays impinging after penetration through the walls. The received power is significantly lower than in area $\mathcal{A}$, and the spatial variation of the signal power is higher.
- In the area $\mathcal{C}$ most of the signal power arrives after penetration through the wall or window followed by some reflections and diffractions. The spatial variation is higher than in areas $\mathcal{A}$ and $\mathcal{B}$.

The WinProp is used to obtain the information on the incoming signal components with a resolution of $8\,\mathrm{cm}$ in the room. For each point, the IlmProp uses this information to produce the channel impulse responses in a window of size $2\lambda \times 2\lambda$ by using a Uniform Rectangular Array (URA) of size 16×16, resulting in 256 subchannels. A temporal variation is included to model man movement . The goal of the simulations is to estimate the possible improvements of the spatio-temporal signal availability when different receive antenna configurations are used.

The following theoretical receiver antennas are studied: vertically polarized dipoles (denoted as 'V'), horizontally polarized dipoles ('H'), a combination of vertically and horizontally polarized dipoles ('V-H'), and circularly polarized

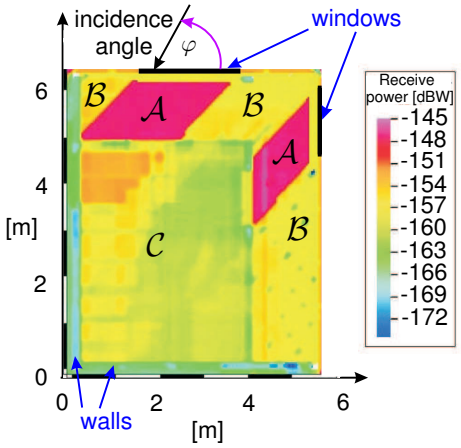

Fig. 2. Average receive power in dBW simulated by WinProp

antennas ('C'). Additionally we study the use of realistic measured vertically ('W') and circularly ('Z') polarized antennas for the reception of satellite signals. The measured vertically polarized antenna has a very narrow radiation pattern with a peak at 40° elevation. Finally, the measured beampatterns of circular antennas with the coupling effect ('CO') are considered. 'CO max' and 'CO min' denote the circular antennas mentioned above having its beampattern maximum and minimum in the LOS direction, respectively. The 3D radiation patterns of the considered antennas are shown in Fig. 3, Fig. 4, and Fig. 5.

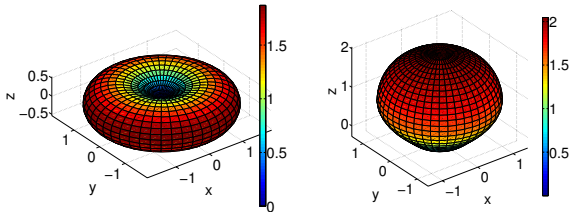

(a) (b)

Fig. 3. Theoretical antenna patterns: (a) vertically / horizontally polarized dipole, (b) circularly polarized antenna

The 3D integral of the radiation patterns is equal to 4π for all studied antennas, i.e.,

$$\int_{S^2} r(\varphi,\theta)\,\mathrm{d}\Omega = 4\pi, \tag{4}$$

where the integral is calculated over the solid angle Ω on the entire surface of the unit sphere S^2.

The receiver is assumed to have a uniform linear array (ULA) with various combinations of the antennas specified above. Antenna arrays of one, two, and four antenna elements are considered at the receiver. The array names give information about its elements, e.g., 'Z-Z' is an ULA of two 'Z' antenna elements, '4-Z' is an ULA of four 'Z' antenna elements, etc. Maximum Ratio Combining (MRC) is performed at the receiver assuming perfect instantaneous channel state information. The transmitted satellite signal is left hand circularly polarized. The penetration losses of the window, brick walls, and the concrete ceiling are 2 dB, 12 dB, and 17 dB, respectively.

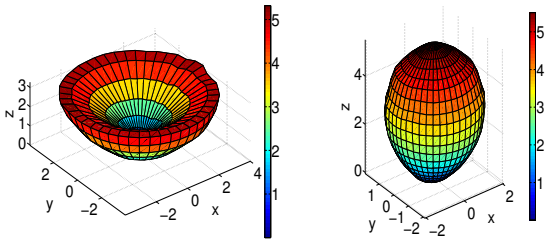

(a) (b)

Fig. 4. Radiation patterns of realistic antennas for the reception of satellite signals: (a) vertically polarized antenna, (b) circularly polarized antenna

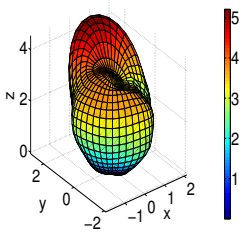

Fig. 5. Radiation pattern of circularly polarized antenna with coupling effect: the distance between identical antenna elements is 0.5 wavelengths.

The correlation coefficient between adjacent antennas is an important metric to observe because it influences the diversity gain and the antenna array gain: low values of the correlation coefficient lead to a high diversity gain and a low array gain, and high values lead to a high array gain and a low diversity gain. The complex correlation coefficient ρ of two complex processes H_1 and H_2 is defined as:

$$\rho = \frac{\mathrm{E}[H_1 H_2^*] - \mathrm{E}[H_1]\mathrm{E}[H_2^*]}{\sqrt{\left(\mathrm{E}\left[H_1 H_1^*\right] - \mathrm{E}[H_1]\mathrm{E}\left[H_1^*\right]\right)\left(\mathrm{E}\left[H_2 H_2^*\right] - \mathrm{E}[H_2]\mathrm{E}\left[H_2^*\right]\right)}}, \tag{5}$$

where $\mathrm{E}[\cdot]$ denotes the expectation operator, H_1 and H_2 obtained from IlmProp simulations are the channels of the first and second antenna, respectively, and $\{\cdot\}^*$ denotes complex conjugation.

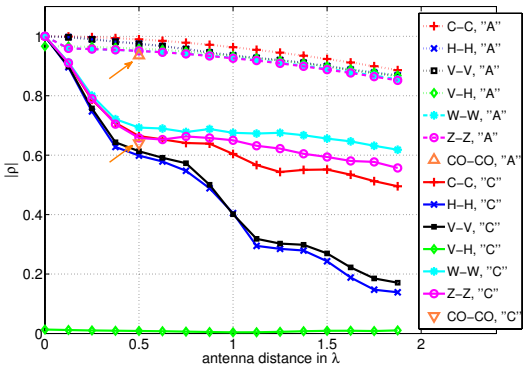

Fig. 6. Averaged spatial correlation coefficient as a function of the distance (in wavelengths) between adjacent antenna elements for different receive antenna schemes in the areas $\mathcal{A}$ and $\mathcal{C}$. The satellite elevation is 40°.

In Fig. 6, the averaged spatial correlation coefficients between different antenna types are depicted as a function of the adjacent antenna distance (in wavelengths) within the area $\mathcal{A}$ and within the area $\mathcal{C}$. For the coupled antennas, only the correlation coefficient for a distance of 0.5 wavelengths is available: we only have measured radiation patterns of coupled antennas for that distance between antenna elements. Since the coupling influence is higher for lower antenna distances between adjacent antenna elements [12], for higher distances the correlation coefficient should approach the correlation coefficient between two measured circularly polarized antennas 'Z-Z'. In Fig. 7 and Fig. 8 the CDF of the fade depth within the whole room for two and four antenna schemes is shown, respectively. For comparison we show also the performance of a receiver with one vertically polarized antenna in both Fig. 7 and Fig. 8. Moreover, figures with the zoomed low and high region of the CDF for all studied two and four receive antenna schemes are shown in Fig. 9 and Fig. 10, respectively.

In the area $\mathcal{A}$, all observed correlation coefficients have very high values that drop slowly with the increase of the distance between antennas. In the area $\mathcal{C}$ the correlation coefficient between two circularly polarized closely spaced antennas ('C-C', 'CO-CO', or 'Z-Z') is higher than for two vertically or two horizontally polarized dipoles with the same separation. The correlation coefficient between one vertically and one horizontally polarized dipole within area $\mathcal{C}$ is very low for all antenna distances. The correlation coefficient within area $\mathcal{A}$ is significantly higher than in area $\mathcal{C}$ for all observed antenna configurations. Therefore and due to the fact that the diversity gain increases at higher availabilities, at lower CDF values of the fade depth the array gain is dominant, while at high CDF values the diversity gain is dominant.

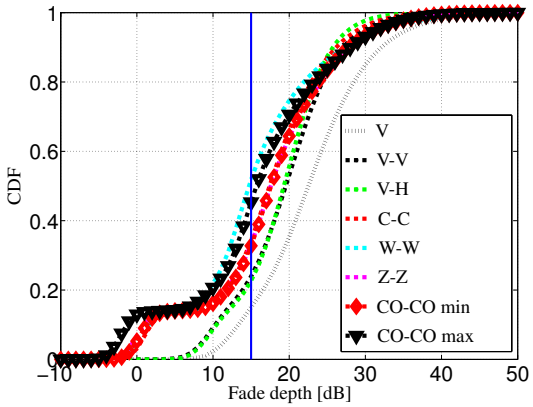

Fig. 7. Cumulative distribution function of the fade depth for two antenna receiver schemes. The satellite elevation is 40°.

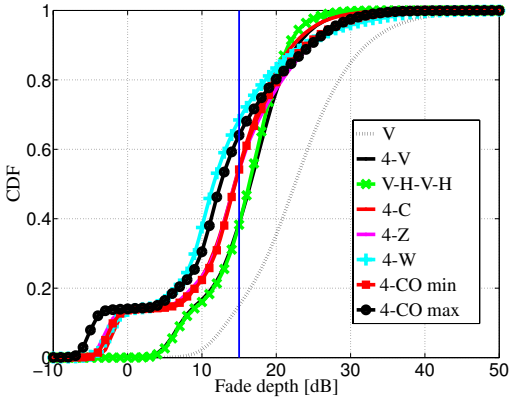

Fig. 8. Cumulative distribution function of the fade depth for four antenna receiver schemes. The satellite elevation is 40°.

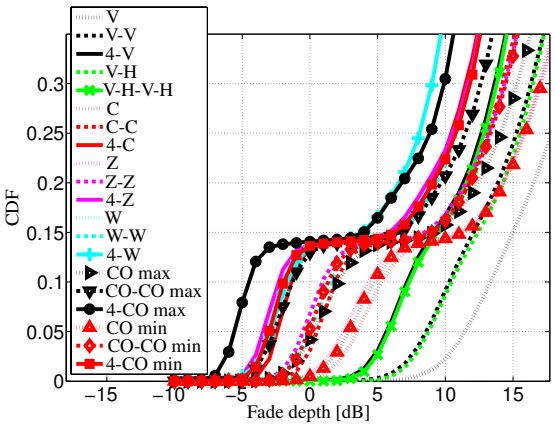

Fig. 9. Zoom of the low CDF region for 40° elevation.

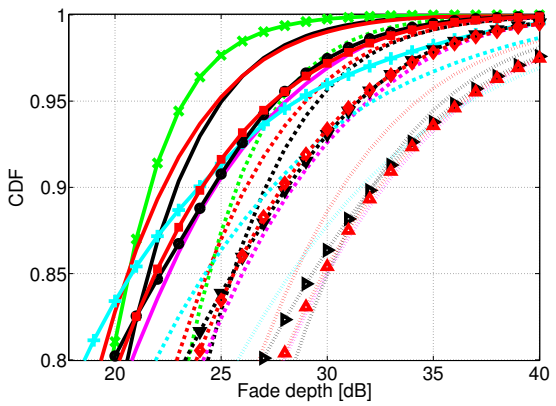

Fig. 10. Zoom of the high CDF region for 40° elevation. The legend is the same as in Fig. 9

For the investigation of the CDF of the fade depth, the distance between adjacent antenna elements is set to half of the wavelength (λ). The combinations of circularly polarized antennas ('4-CO max', '4-Z', '4-C', and '4-CO min') offer the best availability in the area $\mathcal{A}$ (corresponds to the low CDF region in Fig. 8) since they have the same polarization as the transmitted signal and high radiation pattern values at an elevation of 40°. Moreover, the signals between two or more circularly polarized antennas of the same type are highly correlated, introducing an additional array gain at low CDF values. Also the '4-W' array shows a good performance in area $\mathcal{A}$ due to its high radiation pattern values at 40° elevation and the high correlation coefficient. It can be seen that the coupling effect can both improve and decrease the performance depending on the antenna positions and the direction of arrival of the LOS component. This means that in satellite-to-indoor broadcasting a link margin increase is needed to compensate the possible coupling effect if the receiver consists of multiple closely spaced antennas. For very low distances between adjacent antenna elements (lower than half of a wavelength) the other option to compensate coupling is to perform the decoupling at the receiver, as done in [12]. Such a decoupling network performs well only for channels with low bandwidths (on the order of a few percents of the used carrier frequency). At medium CDF values (around 50 %) the '4-W' and '4-CO max' arrays show the best performance. In high availability regimes (region of high CDF values) in Fig. 10 the best performance is achieved with the use of the V-H-V-H array due to its low correlation coefficient and the fact that the diversity gain increases with higher availabilities. At an availability of 99 %, it has a 3 dB gain over the '4-V' and '4-C' array, a 6 dB gain over '4-CO max', and a 7 dB gain over the 'C-C' scheme. It is known from the literature [2] that the link margin of 15 dB is realistic in existing systems. For this link margin (represented with blue vertical lines in Fig. 7 and Fig. 8), the highest availability of 68 % is achieved with the '4-W' array, while the '4-CO max', '4-CO min', and '4-C' antenna configurations have availabilities in the range between 52 % and 64 %. For the antenna configuration 'C-C', the availability within the area $\mathcal{A}$ equals 100 %, within the area $\mathcal{B}$ 39 %, and within the area $\mathcal{C}$ 10 %. Obviously, the best place to put the receiver is just behind the windows, anywhere within the area $\mathcal{A}$. The performance of measured circularly polarized antenna beampattern fits well with the performance of the theoretical circularly polarized antenna beampattern. The impact of the coupling effect is lower for higher availabilities, since in the NLOS area the rays impinge on the receiver from all directions. For the performance of the two antenna receiver schemes depicted in Fig. 7 very similar conclusions can be drawn as for the four antenna receiver schemes.

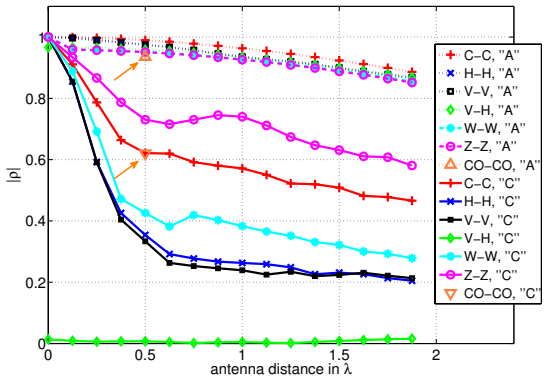

Fig. 11. Averaged spatial correlation coefficient as a function of the distance between adjacent antenna elements for different receive antenna schemes in the areas $\mathcal{A}$ and $\mathcal{C}$. The satellite elevation is 70°.

In Fig. 11, the spatial correlation coefficients between different antenna types within the area $\mathcal{A}$ and within the area $\mathcal{C}$ are shown for a satellite elevation of 70°. In Fig. 12 and Fig. 13 the CDF of the fade depth within the whole room for the two and four antenna schemes is shown, respectively. At higher elevations the size of the area $\mathcal{A}$ decreases. Therefore, the steep increase of the CDF for lower values of the fade depth is significantly reduced. The correlation coefficient between one horizontally and one vertically polarized antenna is very close to zero for all elevations and antenna distances. The correlation coefficients between two horizontally ('H-H'), two vertically ('V-V', 'W-W'), and two circularly polarized antennas ('C-C', 'CO-CO') decrease for 70° satellite elevation if compared to the values for 40° elevation. Therefore, the diversity gain difference between 'V-H-V-H' and other antenna configurations with the same number of elements in middle and high areas of the corresponding CDF

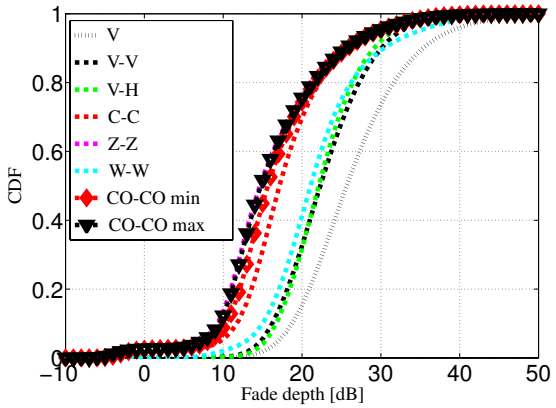

Fig. 12. Cumulative distribution function of the fade depth for two antenna receiver schemes. The satellite elevation is 70°.

of the fade depth is reduced in comparison to the case of 40° elevation.

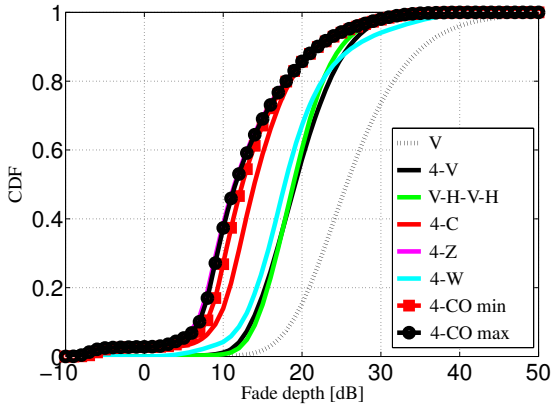

Fig. 13. Cumulative distribution function of the fade depth for four antenna receiver schemes. The satellite elevation is 70°.

The radiation pattern of the circularly polarized antennas ('4-CO max', '4-CO min', '4-C', and '4-Z') at an elevation of 70° is higher than the radiation patterns of vertically or horizontally polarized antennas. Moreover, the diversity gain of 'V-H-V-H' is only slightly higher than the diversity gain of the other four antenna schemes at 70° elevation. These two facts are the reason that the antenna arrays consisting of circularly polarized antennas ('4-CO max', '4-CO min', '4-C', and '4-Z') outperform the other antenna arrays with an equal number of antenna elements at higher elevations for all CDF values. Due to the narrow radiation pattern pointing to elevations close to 40° the arrays consisting of 'W' elements show a poor performance at higher elevations. For the performance of two antenna receiver schemes shown in Fig. 12 similar conclusions can be drawn as for the four antenna receiver schemes.

In Fig. 14, the averaged predicted receive power difference is depicted for a room with and without windows where the receiver has one vertically polarized antenna. The area $\mathcal{A}$ from Fig. 2 does not exist in a room without windows: it transforms into area $\mathcal{B}$ and has significantly lower receive power, on the order of 10 dB. On the other hand, in the area $\mathcal{C}$ there is no significant difference with respect to the averaged received power. Therefore, the removal of the windows decreases significantly the availability for link margins lower than 15 dB, while at higher link margins (higher values in the CDF) this decrease is almost negligible. In other words, if the target availability is very high (e.g., 99%) the existence of the windows is of a rather small significance.

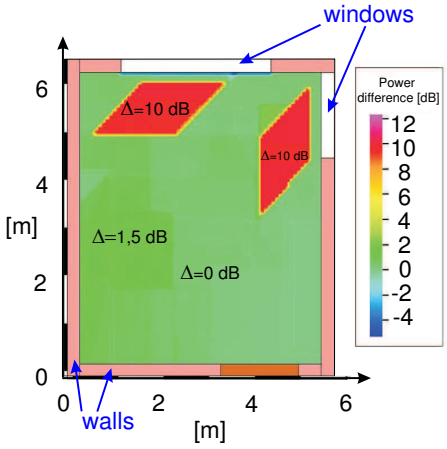

Fig. 14. Averaged received power difference in a room with and without windows, both with the LOS to the satellite.

4. CONCLUSIONS

This paper presents the results of study on the influence of the receive antenna array type on the spatio-temporal availability in satellite-to-indoor broadcasting communications. Numerous antenna array receivers with various polarimetric radiation patterns and coupling effect are compared for different satellite elevation angles. The study is carried out on the basis of a 3D ray tracing engine and of a geometry-based channel modeling tool. The developed flexible test-bed for a satellite-to-indoor system is able to predict the link margin required to achieve target availability. Additional antennas placed at the receiver reduce the spatio-temporal variability of the channel, and therefore improve the system performance. In the LOS

areas, the best performance is achieved by multiple circularly polarized receive antennas, whereas in the NLOS areas, a combination of horizontally and vertically polarized antennas is a good candidate, especially if very high availabilities are considered. Moreover, the influence of coupling effect between closely spaced antennas on the availability is studied. The antenna coupling effect can both increase or decrease the system performance, depending on the distance between adjacent antenna elements, and the orientation of the receive antenna array. In general, the harmful antenna coupling effects should be handled by increasing the needed link margin or by performing the decoupling at the receiver. Also, the performance in rooms with and without windows is compared for a LOS connection to the satellite: the windows cause a significant performance difference in the LOS area of the room while outside of it the impact is not significant.

5. REFERENCES

[1] F. Pérez-Fontán, B. Sanmartín, A. Steingaß, A. Lehner, J. Selva, E. Kubista, and B. Arbesser-Rastburg, "Measurements and modeling of the satellite-to-indoor channel for Galileo," in *European Navigation Conference GNSS 2004*, Rotterdam, The Netherlands, May 2004.

[2] T. Heyn and C. Wagner, "Propagation channel characterisation - Final report," IST Integrated Project No 507023 - MAESTRO, Jan. 2005.

[3] T. Heyn, A. Heuberger, and C. Keip, "Propagation measurements for the characterisation of a hybrid mobile channel in S-band," in *Proc. IST Mobile Summit Conference*, Dresden, Germany, June 2005.

[4] B. G. Molnár, I. Frigyes, Z. Bodnár, Z. Herczku, Zs. Kormányos, J. Bérces, I. Papp, and L. Juhász, "A detailed experimental study of the LEO satellite to indoor channel characteristics," *International Journal of Wireless Information Networks*, April 1999.

[5] L. Farkas and L. Nagy, "Satellite-to-indoor wave propagation channel simulation. First results - the polarization characteristics of the indoor wave," *Personal, Indoor and Mobile Radio Communications, PIMRC'2000*, Sept. 2000.

[6] N. Song, G. Del Galdo, M. Milojević, M. Haardt, and A. Heuberger, "Spatial availability in satellite-to-indoor broadcasting communications," in *Proc. 7th Workshop Digital Broadcasting*, Erlangen, Germany, Sept. 2006, pp. 113–118.

[7] M. Milojević, G. Del Galdo, N. Song, M. Haardt, and A. Heuberger, "Spatio-temporal availability in satellite-to-indoor broadcasting," in *European Conference on Wireless Technology (ECWT2007)*, Munich, Germany, 2007.

[8] G. Del Galdo, *Geometry-based Channel Modeling for Multi-User MIMO Systems and Applications*, Ph.D. thesis, Ilmenau University of Technology, Ilmenau, Germany, ISBN: 978-3-938843-27-7, available to download at http://www.delgaldo.com.

[9] G. Wölfle, B. E. Gschwendtner, and F. M. Landstorfer, "Intelligent ray tracing - A new approach for the field strength prediction in microcells," *47th Vehicular Technology Conference (VTC) 1997*, May 1997.

[10] R. Hoppe, T. Hager, T. Heyn, A. Heuberger, and H. Widmer, "Simulation and measurement of the satellite to indoor propagation channel at L- and S-band," in *Proc. EuCAP 2006*, France, Nice, Nov. 2006.

[11] G. Wölfle, R. Hoppe, and F. M. Landstorfer, "A fast and enhanced ray optical propagation model for indoor and urban scenarios, based on an intelligent preprocessing of the database," in *Proceedings of the 10th IEEE International Symposium on Personal, Indoor and Mobile Radio Communications (PIMRC)*, Osaka, Japan, Sept. 1999.

[12] C. Volmer, J. Weber, R. Stephan, K. Blau, and M. A. Hein, "An eigenanalysis of compact antenna arrays and its application to port decoupling," *IEEE Transactions on Antennas and Propagation*, vol. 56, Feb. 2008.